Cellular/Molecular

Energy Contribution of Octanoate to Intact Rat Brain Metabolism Measured by ^{13}C Nuclear Magnetic Resonance Spectroscopy

Douglas Ebert,[1] Ronald G. Haller,[1,2,3] and Marlei E. Walton[1]

[1]Veterans Affairs North Texas Health Care System, Dallas, Texas 75216, [2]Department of Neurology, University of Texas Southwestern Medical Center, Dallas, Texas 75235, and [3]Institute for Exercise and Environmental Medicine, Presbyterian Hospital of Dallas, Dallas, Texas 75231

Glucose is the dominant oxidative fuel for brain, but studies have indicated that fatty acids are used by brain as well. We postulated that fatty acid oxidation in brain could contribute significantly to overall energy usage and account for non-glucose-derived energy production. [2,4,6,8-$^{13}C_4$]octanoate oxidation in intact rats was determined by nuclear magnetic resonance spectroscopy. We found that oxidation of ^{13}C-octanoate in brain is avid and contributes ~20% to total brain oxidative energy production. Labeling patterns of glutamate and glutamine were distinct, and analysis of these metabolites indicated compartmentalized oxidation of octanoate in brain. Examination of liver and blood spectra revealed that label from ^{13}C-octanoate was incorporated into glucose and ketones, which enabled calculation of its overall energy contribution to brain metabolism: glucose (predominantly unlabeled) and ^{13}C-labeled octanoate can account for the entire oxidative metabolism of brain. Additionally, flux through anaplerotic pathways relative to tricarboxylic acid cycle flux (*Y*) was calculated to be 0.08 ± 0.039 in brain, indicating that anaplerotic flux is significant and should be considered when assessing brain metabolism. *Y* was associated with the glutamine synthesis compartment, consistent with the view that anaplerotic flux occurs primarily in astrocytes.

Key words: **metabolism; brain; glutamate; glutamine; glucose; NMR; ^{13}C spectroscopy**

Introduction

Glucose is well established as the major oxidative fuel for brain (Sokoloff et al., 1977), but cell culture (Edmond et al., 1987; Auestad et al., 1991) and *in vivo* (Cerdan et al., 1990; Kuge et al., 1995; Lebon et al., 2002) experiments have demonstrated that fatty acids are oxidized by brain tissue as well. Cell culture studies with astrocytes, neurons, and cocultures of these cells have ascertained that fatty acid metabolism in brain occurs in astrocytes (Edmond et al., 1987; Waniewski and Martin, 1998). Moreover, these cells prefer fatty acids to glucose as an oxidative fuel (Edmond et al., 1987).

We hypothesized that fatty acid oxidation in brain could contribute significantly to overall energy usage. Previous studies of fat oxidation in brain have been limited to acetate, the simplest of fats (Badar-Goffer et al., 1990; Cerdan et al., 1990; Hassel and Sonnewald, 1995; Sonnewald et al., 1996; Lebon et al., 2002); however, acetate is not a primary physiological fuel for brain (Vannucci and Hawkins, 1983; Edmond, 1992). Conversely, octanoate is a medium-chain fatty acid that composes up to 13% of the normal free fatty acid pool in humans (Mamunes et al., 1974), readily crosses the blood–brain barrier (Oldendorf, 1971, 1973), and is an important component of medium-chain triglycerides used in various clinical settings (Sulkers et al., 1989; Eckel et al., 1992; Rouis et al., 1997; Gillingham et al., 1999). Octanoate may also offer a unique approach to dissecting the glutamate–glutamine neurotransmitter cycle on the basis of evidence that fatty acid oxidation (Edmond et al., 1987) as well as glutamine synthesis (Norenberg and Martinez-Hernandez, 1979) occur predominantly in astrocytes. We therefore examined ^{13}C-labeled octanoate to more fully understand the biochemistry of this medium-chain fatty acid in brain in the intact animal.

Materials and Methods

Animal preparation and experimental design. All experimental procedures were approved by the Institutional Animal Care and Use Committee at the Veterans Affairs North Texas Health Care System (VANTHCS). Adult male Sprague Dawley rats (329.1 ± 10.6 gm; Charles River, Kingston, MA) were housed in the VANTHCS Animal Resources Center with a 12 hr light/dark cycle and had *ad libitum* access to water and lab chow.

Rats were weighed and anesthetized with an intraperitoneal injection of 1–3 ml/kg ketamine/xylazine mixture (6 mg/ml xylazine, 94 mg/ml ketamine). After a tracheotomy was performed, 1–2.5% isoflurane (Isotec 3 vaporizer, Matrix Medical, Buffalo, NY) in 100% O_2 was used to maintain anesthesia and delivered via a positive-pressure ventilator (model 683 Small Animal Ventilator, Harvard Apparatus, South Natick, MA) at a rate of 1.25 cc/min, ~100 breaths per minute. The right carotid artery was catheterized and connected to a fluid-filled pressure transducer (model P23XL Gould Transducer, Future Tech, Birmingham, AL)

Received Oct. 10, 2002; revised March 4, 2003; accepted April 18, 2003.

This study was supported by Veterans Affairs Merit Grant 98-139 and Veterans Integrated Service Network17 Grant 99-89. We thank Drs. Mark Jeffrey and Craig Malloy for constructive conversations regarding this work and gratefully acknowledge the laboratory of Dr. Henri Brunengraber for measurement of octanoate concentrations and enrichments.

Correspondence should be addressed to Douglas Ebert, Veterans Affairs North Texas Health Care System, 4500 South Lancaster Road (151), Dallas, TX 75216. E-mail: mwde@swbell.net.

 0270-6474/03/235928-08$15.00/0

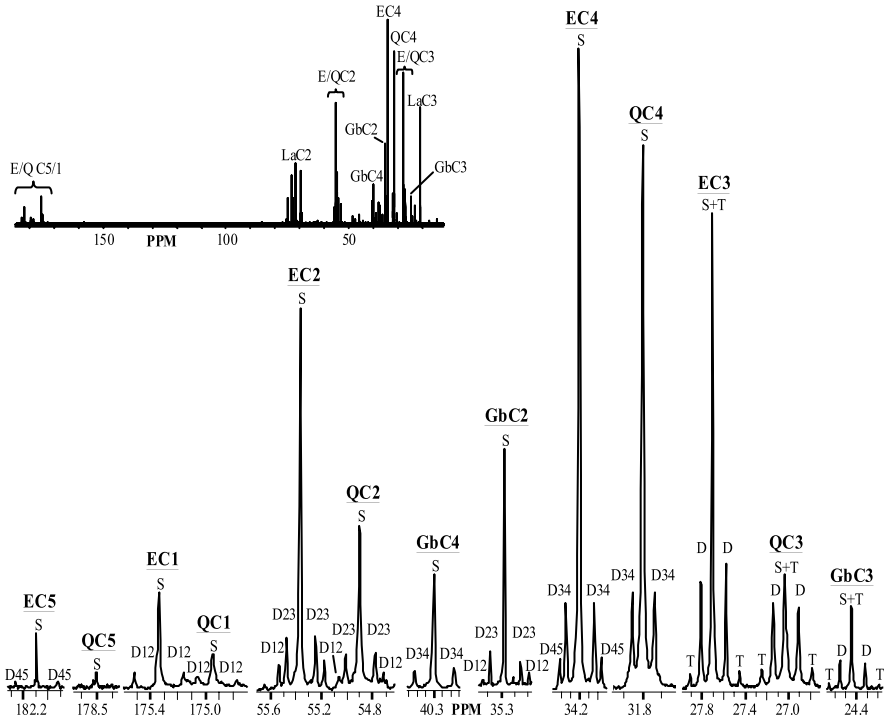

Figure 1. ^{13}C spectrum of representative extract of intact rat brain infused with [2,4,6,8-$^{13}C_4$]octanoate for 105 min. Glutamate (E) and glutamine (Q) regions of carbons 1–5 (C1–C5) and GABA (Gb) C2–C4 are shown. Multiplets are depicted as follows: singlet (S), doublet (D), and triplet (T). Doublets resulting from carbon–carbon coupling of adjacent carbons are noted [e.g., C3 and C4 (D34) in C4 region]. Inset, Full ^{13}C spectrum; regions of E, Q, Gb, and lactate (La) carbon resonances are indicated. PPM, Parts per million.

to continuously monitor heart rate and blood pressure throughout the surgical procedure. Systemic arterial blood gases were monitored using a blood gas analyzer (ABL-4, Radiometer, Westlake, OH). Gas mixture and ventilation rate were adjusted to maintain physiological blood pH (end pH 7.3 ± 0.10) and arterial O_2 saturation to 99+%. After arterial cannulation, the jugular vein was cannulated and connected to an infusion pump (model 22, Harvard Apparatus) for administration of labeled and unlabeled octanoate. Initially, 220 mM unlabeled sodium octanoate (Aldrich, Milwaukee, WI) was infused at a rate of 2.67 ml/hr. Temperature was maintained at 37°C with an external heating pad under the rat in combination with heat radiating from an incandescent light source illuminating the surgical field.

At time 0 (after ~30 min of unlabeled octanoate infusion), infusate was changed to 220 mM sodium [2,4,6,8-$^{13}C_4$]octanoate (Cambridge Isotope Laboratories, Andover, MA). Additionally at time 0, muscles of the left limb were contracted via direct electrical stimulation to the sciatic nerve. After 105 min of ^{13}C-octanoate infusion, a blood sample was taken, and tissues including whole brain (forebrain, cerebellum, and brainstem) and liver were surgically isolated, immediately frozen in liquid nitrogen, and then stored at −80°C until extraction. The rat was killed by removal of the heart under deep anesthesia.

Tissue preparation. Whole brain and liver were extracted by homogenization in ice-cold 3.6% perchloric acid (PCA) with a motor-driven tissue grinder (model 985–370, Biospec Products, Bartlesville, OK). Brain and liver homogenates and PCA-extracted blood samples were then centrifuged, neutralized, and lyophilized overnight in a rotary evaporator (SpeedVac, Savant Instruments, Farmingdale, NY; Flexi-Dry microprocessor lyophilizer, FTS Systems, Stone Ridge, NY). Lyophilates were brought to a volume of 550 μl in deuterium oxide (Cambridge Isotope Laboratories).

Metabolite concentration. Aliquots (150 μl) of arterial blood taken from the carotid artery were obtained before octanoate infusion and at the end of the experiment. Plasma was analyzed using gas chromatography–mass spectrometry to determine enrichment and concentration of octanoate at these time points (Powers et al., 1995). Octanoate was assayed by derivatization with 2,4-difluoroaniline, using 1,3-dicyclohexylcarbodiimide as a coupling agent. [9,9,9-$^2H_3$]nonanoate was used as an internal standard. Additionally, glucose and ketones (acetoacetate and β-hydroxybutyrate) were measured fluorometrically (Maughan, 1982) from a 40 μl aliquot of arterial blood.

Nuclear magnetic resonance spectroscopy. Proton-decoupled ^{13}C and solvent-suppressed ^1H nuclear magnetic resonance (NMR) spectra of the tissue extracts were collected at 37°C on a Varian INOVA 600 MHz spectrometer (Varian, Palo Alto, CA) in a 5 mm broadband probe. ^{13}C NMR spectra were obtained using a 30 K sweep width, 45° pulse, 1.5 sec pulse delay, and bilevel proton decoupling. To achieve adequate signal to noise, the number of scans acquired was typically 4000 for brain and 1000 for liver and blood. Solvent-suppressed ^1H spectra were collected with a pulse width of 9.2 μsec, 10 sec pulse delay, and 32 scans per sample. Free induction decays were baseline corrected and multiplied by an exponential function before Fourier transformation; 0.5 Hz line broadening was used for all extracts. Areas and intensities of ^{13}C and ^1H spectra were quantitated by a curve-fitting program (NUTS, Acorn Inc.). Line fit was considered adequate if difference spectra were indistinguishable from spectral regions with no visible peaks. For ^{13}C glutamate and glutamine regions, each multiplet area was normalized and reported as a fraction of the total area for that specific carbon resonance.

Data analysis. Acetyl-CoA fractional enrichments were determined by non-steady-state and steady-state isotopomer analysis (Malloy et al., 1987, 1988, 1990). Flux through combined anaplerotic reactions relative to tricarboxylic acid (TCA) cycle flux (Y) was determined by steady-state isotopomer analysis (Malloy et al., 1987, 1988). Isotopomer analysis is based on evolution of ^{13}C label in metabolites in exchange with the TCA cycle. Acetyl-CoA fractional enrichments and Y can be ascertained from ^{13}C spectra by determining (1) the fractional contribution of glutamate and glutamine multiplet areas within a given carbon resonance and (2) the ratios of all peak areas in different carbons. The fractional contribution of acetyl-CoA labeled only in carbon 2 to the entire acetyl-CoA pool is designated Fc2; the contribution of acetyl-CoA labeled only in carbon 1, Fc1; contribution of doubly labeled acetyl-CoA, Fc12; and Fc0 represents the unlabeled fraction of the acetyl-CoA pool from unlabeled sources. We used non-steady-state equations from Malloy et al. (1990) to calculate Fc2 and Fc0. Steady-state values were obtained using TCAcalc (http://www2.swmed.edu/rogersmr/availableproducts.htm), a program that analyzes a set of simultaneous nonlinear equations to solve for relative fluxes through pathways intersecting the TCA cycle (Malloy et al., 1988; Jeffrey et al., 1996).

Isotopic steady state was determined by comparing (1) spectral versus steady-state-calculated peak areas and (2) fractional enrichment values using non-steady-state (Malloy et al., 1990) versus steady-state (Malloy et al., 1987) equations. Brain metabolism was modeled using steady-state analysis results from liver as well as TCAsim software (http://www2.swmed.edu/rogersmr/available__products.htm) (Jeffrey et al., 1991). Results are reported as means ± SD ($n = 5$). The Student's unpaired two-tailed t test was used to compare all measured data; $p \leq 0.01$.

Results

Incorporation of [2,4,6,8-$^{13}C_4$]octanoate in brain

A representative ^{13}C spectrum of the extract of whole brain from rats infused with [2,4,6,8-$^{13}C_4$]octanoate for 105 min is shown in Figure 1. The inset shows resonance regions from all five glutamate (E) and glutamine (Q) carbons 1–5 (C1–C5) and GABA

Table 1. Glutamate and glutamine isotopomer analysis

	Glutamate		Glutamine	
	NSS	SS	NSS	SS
Fc2	0.227 ± 0.030	0.227 ± 0.021	0.656 ± 0.079*	0.558 ± 0.039*
Fc0	0.773 ± 0.030	0.734 ± 0.027	0.344 ± 0.079*	0.405 ± 0.031*
Fc1		0.030 ± 0.020		0.031 ± 0.015
Fc12		0.010 ± 0.005		0.006 ± 0.007
Y		0.080 ± 0.039		0.658 ± 0.075*

Results of non-steady-state (NSS) and steady-state (SS) isotopomer analysis of glutamate and glutamine listed as mean ± SD ($n = 5$). Fc2 represents the fraction of acetyl-CoA labeled in the carbon 2 (C2) position, predominantly from exogenous [2,4,6,8–$^{13}C_4$]octanoate; Fc0 corresponds to the contribution of unlabeled acetyl-CoA from unlabeled endogenous substrates; Fc1 and Fc12 show the fraction of acetyl-CoA labeled in C1 and both C1 and C2, respectively; and *Y* depicts flux through anaplerotic pathways relative to TCA cycle flux. No differences were found between non-steady-state and steady-state values for either glutamate or glutamine; *different from glutamate ($p \leq 0.01$).

carbons C2–C4 (Fig. 1). ^{13}C-labeled octanoate is avidly metabolized by brain, resulting in multiple peaks (multiplets) in each of these resonance areas.

Incorporation of ^{13}C-labeled octanoate in brain results in different labeling patterns between corresponding glutamate and GABA versus glutamine carbons (Fig. 1). The labeling pattern of GABA most closely resembles that of glutamate, as evidenced by a much higher singlet to doublet ratio in GABA and glutamate C3 as compared with glutamine C3 (Fig. 1). In the glutamine C4 region, there is a conspicuous lack of a doublet arising from C4–C5 carbon–carbon coupling (D45) that is clearly present in the glutamate C4 and GABA C2 resonances (Fig. 1). In fact, in both C4 and C5 of glutamate, D45 is readily apparent (Fig. 1).

Glutamate and glutamine isotopomer analysis in brain

Relative peak areas and ratios from glutamate and glutamine resonances are used in steady-state and non-steady-state calculations of fractional contributions to acetyl-CoA in brain. No differences were found in spectral data compared with calculated steady-state values for either glutamate or glutamine. Additionally, non-steady-state analysis was used as a tool to determine whether steady state had been achieved in these experiments. Fc2 values from non-steady-state versus steady-state analysis were not different for either glutamate or glutamine (Table 1). These data indicate that glutamate and glutamine isotopic steady state (ISS) had been reached by 105 min.

Glutamate steady-state Fc2 values (Table 1) indicated significant oxidation of medium-chain fatty acid by brain TCA cycle. Twenty-three percent of acetyl-CoA in brain was enriched by infusion with [2,4,6,8-$^{13}C_4$]octanoate. Glutamine steady-state isotopomer analysis (Table 1) yielded a higher Fc2 value of 56%. Values for both glutamate and glutamine represent substantial oxidation of fatty acid within brain tissue, and disparate distribution of octanoate-derived label among TCA cycle ancillary reactions indicates a compartmentation of octanoate metabolism within brain.

Because ISS was achieved in these experiments, it was possible to calculate flux through anaplerotic pathways relative to TCA cycle flux (*Y*) in the brain (Table 1). *Y* is higher in glutamine versus glutamate isotopomer analysis (Table 1), indicating that most of the anaplerotic flux in brain is occurring in the TCA cycle associated with glutamine production. The percentage of glutamate and glutamine metabolite pools generated through anaplerotic pathways can be calculated using the equation $Y/(Y + 1)$ when the TCA cycle flux is set to 1 (Malloy et al., 1988) and the *Y* value for glutamate or glutamine is used (Table 1). The anaplerotic contribution to the glutamate pool (7.3 ± 3.4%) is substantially lower than that of glutamine (39.6 ± 2.6%) in brain.

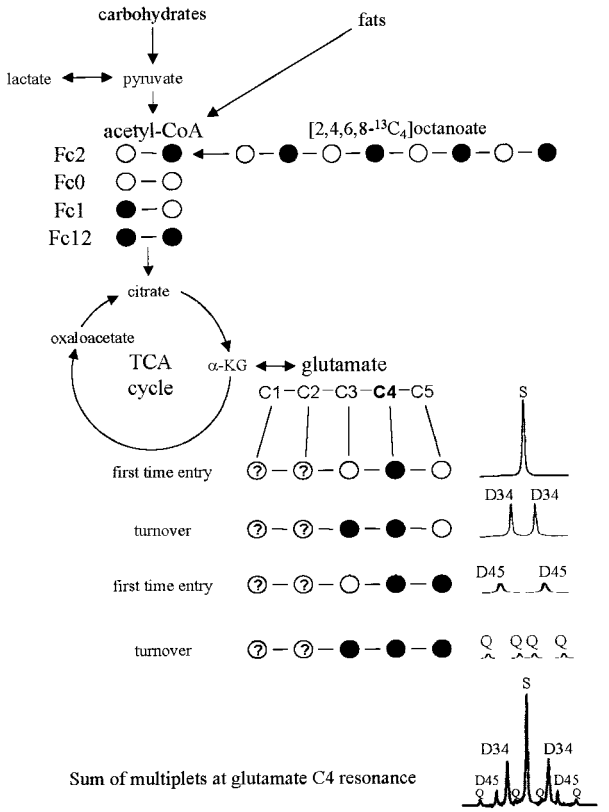

Figure 2. ^{13}C isotope isomer (isotopomer) analysis is based on the appearance of ^{13}C label (●) in the carbons of glutamate originating from labeled acetyl-CoA. Glutamate is in rapid exchange with the TCA cycle intermediate, α-ketoglutarate (α-KG), and is present in concentrations high enough to be readily detected using magnetic resonance spectroscopy. Label from β-oxidation of exogenously administered [2,4,6,8-$^{13}C_4$]octanoate gives rise to label in the carbon 2 of acetyl-CoA (Fc2). When this label enters the TCA cycle the first time, it gives rise to a single peak (singlet) in the glutamate carbon 4 (C4) region. As the TCA cycle turns over, ^{13}C label is mixed at symmetrical intermediates giving rise to label in adjacent carbons, which splits the signal of those carbons into multiple peaks (multiplets). For example, if C2-labeled oxaloacetate condenses with methyl-labeled acetyl-CoA (from exogenous octanoate), a doublet (D34) will be seen (attributable to J34) in the area where glutamate C4 resonates in the ^{13}C spectrum as shown. Different starting populations of labeled acetyl-CoA yield distinct glutamate labeling patterns. If the glutamate C4 resonance is considered, doubly labeled acetyl-CoA first gives rise to D45 in this region. As the TCA cycle turns over and this ^{13}C label is mixed, it is possible to generate label in carbons 3, 4, and 5 of glutamate, leading to a doublet of doublets or quartet (Q) in the glutamate C4 resonance. No label is generated in the C4 area from the unlabeled acetyl-CoA populations (Fc0) or those labeled only in carbon 1 (Fc1). Thus, the combination of the S, D34, D45, and Q in the glutamate C4 region will be nine peaks. This analysis can be done with other carbons of glutamate (e.g., C3) or other metabolites (e.g., glucose).

Contribution of ^{13}C-labeled glucose to brain metabolism

[2,4,6,8-$^{13}C_4$]octanoate administered in these experiments can only provide acetyl-CoA units labeled in carbon 2 (Fc2) (Fig. 2). Glutamate molecules labeled in both the 4 and 5 positions can only arise from a substrate that provides doubly labeled acetyl-CoA (Fc12) (Fig. 2). Thus exogenously administered ^{13}C-labeled octanoate must have been metabolized elsewhere in the animal, and ^{13}C label redistributed into a substrate that would be available for oxidation in brain. We therefore investigated glucose labeling via gluconeogenesis, as well as the possibility of label arising from ketogenesis.

Octanoate, glucose, and ketones were measured from arterial blood samples taken before octanoate infusion began and at the end of the experiment. Glucose concentration was not different between these two time points (11.4 ± 1.7 mM initial; 11.1 ± 2.7

mM final). Initial ketone levels (acetoacetate plus β-hydroxybutyrate) were 131.2 ± 78.4 μM and increased to a final concentration of 357.4 ± 97.8 μM. Endogenous octanoate was undetectable. After 105 min of infusion with [2,4,6,8-$^{13}C_4$]octanoate, ^{13}C-labeled octanoate concentration was 250 ± 25 μM and unlabeled octanoate was undetectable, indicating nearly 100% octanoate enrichment.

Liver extracts were examined using ^{13}C magnetic resonance spectroscopy. Glutamate steady-state analysis of livers from animals infused for 105 min revealed that the fractional contribution of [2,4,6,8-$^{13}C_4$]octanoate to acetyl-CoA was 40% and *Y* was 37%. To evaluate glucose and ketone ^{13}C labeling, ^{1}H spectra were analyzed to obtain the fractional ^{13}C enrichment of glucose and β-hydroxybutyrate in blood and liver. Carbon 1 of glucose and carbon 4 of β-hydroxybutyrate were chosen as a basis for measuring glucose and β-hydroxybutyrate ^{13}C enrichment because of the absence of interfering resonances in those regions of the ^{1}H spectrum. Areas under side peaks caused by ^{13}C splitting were measured and expressed as a fraction of total peak area in glucose C1 and β-hydroxybutyrate C4 regions. Blood enrichment of glucose C1 reflected that of liver (4.4 ± 1.0%). ^{13}C enrichment of β-hydroxybutyrate C4 in blood was 22.6 ± 8.1%.

To verify that Fc1 and Fc12 in brain (Table 1) were caused by labeled glucose arising from gluconeogenesis, correlating carbons were compared. Glucose C1 enrichment ratios from liver and resultant lactate C3 enrichment ratios in brain were measured and compared with brain acetyl-CoA isotopomers labeled in carbon 1 only and labeled in both carbons 1 and 2 (i.e., the fractional contributions that could not have arisen from ^{13}C-labeled octanoate).

Both α and β anomers of glucose C1 are easily analyzed in ^{13}C spectra. By measuring the doublet resulting from C1 and C2 coupling (D12) and singlet (S) in this region, the relative contribution of glucose isotopomers enriched in both C1 and C2 to the total C1 resonance can be calculated using the ratio D12/(S + D12) (Fig. 3). Through glycolysis, lactate C3 is derived directly from glucose C1 (and C6, which should reflect labeling identical to that of C1), and hence the ratio of D23/(S + D23) in the lactate C3 region was measured in ^{13}C brain spectra (Fig. 3). Lactate D23/(S + D23) is not different from the D12/(S + D12) ratio of the α or β anomer of glucose (Fig. 3). Additionally, overall ^{13}C enrichment of lactate C3 in brain ^{1}H spectra was measured by comparing ^{13}C side peaks with the ^{12}C peak. Fractional enrichment of lactate C3 was 0.040 ± 0.008, which is not different from the 0.044 ± 0.01 enrichment observed in glucose C1.

Similarly, from steady-state glutamate analysis in brain (Table 1), the ratio of doubly labeled (Fc12) and carbon 1-labeled (Fc1 + Fc12) acetyl-CoA pool could be compared with those ratios in the correlating C1 resonance of glucose and C3 resonance of lactate (Fig. 3). Fc12/(Fc1 + Fc12) is not different from D12/(S + D12) for either anomer of glucose in liver, nor is it different from the lactate D23/(S + D23) ratio in brain (Fig. 3).

Fc1 and Fc12 agree well with a contribution of glucose from liver gluconeogenesis to energy metabolism in brain. However, Fc2 is proportionately much larger because of avid oxidation of octanoate in brain. Assuming randomization of label at succinate and fumarate, labeled glucose produced in these experiments will give rise to approximately equal amounts of singly enriched glucose molecules in C1, C2, C5, and C6. Therefore, Fc2 arising from glucose C1 and C6 will be approximately equal to Fc1 arising from glucose C2 and C5. Subtracting the Fc2 contribution from glucose (0.030) from the total Fc2 (0.227) (Table 1) leaves an Fc2 of ~20% attributable to ^{13}C-octanoate.

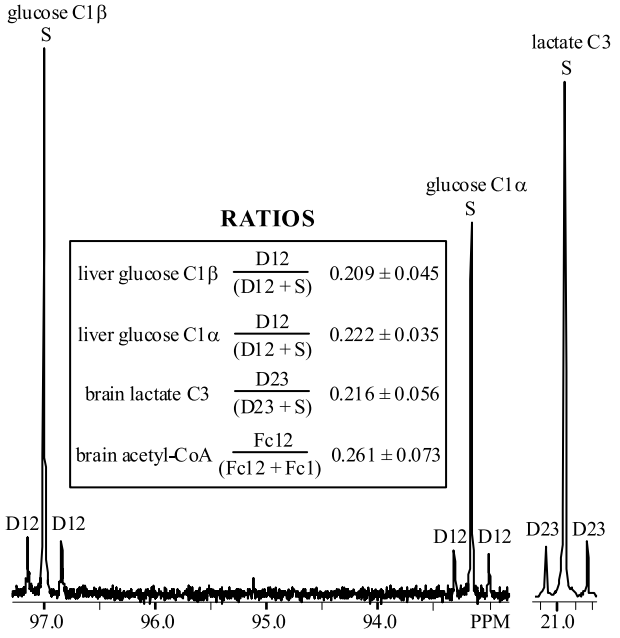

Figure 3. ^{13}C spectral regions of glucose carbon 1 (C1) α and β anomers from representative liver extract and lactate C3 from representative brain extract of intact rat infused with [2,4,6,8-$^{13}C_4$]octanoate for 105 min. Fractional contribution of glucose doublet arising from carbon–carbon coupling of C1 and C2 (D12) is shown in the inset for each anomer. The fractional contribution of the corresponding lactate doublet (D23) and the ratio of the analogous contribution of doubly labeled acetyl-CoA population (Fc12) to acetyl-CoA pool labeled in C1 (Fc1) plus Fc12 in brain is depicted. None of these ratios were different from each other ($p \leq 0.01$).

N-acetyl aspartate enrichment

Brain ^{1}H spectra were analyzed to determine ^{13}C fractional enrichment of *N*-acetyl aspartate (NAA). NAA C6 (corresponding to the methyl carbon of acetyl-CoA) enrichment was 8.5 ± 3.4%. This is not different from fractional enrichment of lactate C3 (4.0%) or of acetyl-CoA C2 (arising from glucose) in brain (Fc2 + Fc12 = 3.9 ± 2.5%) and is consistent with the contribution of enriched ^{13}C-glucose to neuronal acetyl-CoA.

Model of brain metabolism

To verify isotopic distribution of glucose, we constructed a substrate oxidation model based on our data and TCAsim software. With metabolic information about liver in these experiments, it is possible to predict the distribution of the 64 different glucose isotopomers generated via gluconeogenesis using TCAsim (Fig. 4*A*, columns 1, 2). Isotopomer analysis clearly showed a high level of enrichment from a labeled substrate that enriched acetyl-CoA at carbon 2 (Table 1), consistent with [2,4,6,8-$^{13}C_4$]octanoate that was administered. On the basis of the measured Fc2 (0.227) and glucose contribution to Fc2 (0.030), octanoate contribution was calculated to be 20% (Table 1). Because it is well established that glucose is the major oxidative fuel in brain and 20% of metabolism had already been accounted for, 80% of oxidative metabolism was ascribed to glucose (Fig. 4*A*, column 3). The contribution of glucose isotopomers to acetyl-CoA in brain (Fc1, Fc2, Fc12, and Fc0) was calculated by adding all of these isotopomers (Fig. 4*A*, columns Fc1–Fc0). This allows direct comparison of model values with experimental fractional contributions obtained via glutamate isotopomer analysis (Fig. 4*B*, Table 1); they are in precise agreement.

A

Isotopomers	FC	80%FC	Brain acetyl-CoA from 80%FC Fc1	Fc2	Fc12	Fc0
○○○○○○	0.86590	0.69272				0.69272
●○○○○○	0.01547	0.01238		0.00619		0.00619
○●○○○○	0.01643	0.01314	0.00657			0.00657
●●○○○○	0.00643	0.00514			0.00257	0.00257
○○●○○○	0.00408	0.00327				0.00327
●○●○○○	0.00266	0.00213		0.00106		0.00106
○●●○○○	0.00169	0.00136	0.00068			0.00068
●●●○○○	0.00111	0.00089			0.00045	0.00045
○○○●○○	0.00408	0.00327				0.00327
●○○●○○	0.00107	0.00086		0.00043		0.00043
○●○●○○	0.00113	0.00091	0.00045			0.00045
●●○●○○	0.00045	0.00036			0.00018	0.00018
○○●●○○	0.00030	0.00024				0.00024
●○●●○○	0.00019	0.00015		0.00008		0.00008
○●●●○○	0.00013	0.00010	0.00005			0.00005
●●●●○○	0.00008	0.00007			0.00003	0.00003
○○○○●○	0.01643	0.01314	0.00657			0.00657
●○○○●○	0.00418	0.00334	0.00167	0.00167		
○●○○●○	0.00443	0.00354	0.00354			
●●○○●○	0.00176	0.00141	0.00070		0.00070	
○○●○●○	0.00113	0.00091	0.00045			0.00045
●○●○●○	0.00072	0.00058	0.00029	0.00029		
○●●○●○	0.00048	0.00038	0.00038			
●●●○●○	0.00031	0.00025	0.00012		0.00012	
○○○●●○	0.00169	0.00136	0.00068			0.00068
●○○●●○	0.00045	0.00036	0.00018	0.00018		
○●○●●○	0.00048	0.00038	0.00038			
●●○●●○	0.00020	0.00016	0.00008		0.00008	
○○●●●○	0.00013	0.00010	0.00005			0.00005
●○●●●○	0.00008	0.00007	0.00003	0.00003		
○●●●●○	0.00006	0.00005	0.00005			
●●●●●○	0.00004	0.00003	0.00001		0.00001	
○○○○○●	0.01547	0.01238		0.00619		0.00619
●○○○○●	0.00395	0.00316		0.00316		
○●○○○●	0.00418	0.00334	0.00167	0.00167		
●●○○○●	0.00166	0.00133		0.00066	0.00066	
○○●○○●	0.00107	0.00086		0.00043		0.00043
●○●○○●	0.00068	0.00055		0.00055		
○●●○○●	0.00045	0.00036	0.00018	0.00018		
●●●○○●	0.00029	0.00023		0.00012	0.00012	
○○○●○●	0.00266	0.00213		0.00106		0.00106
●○○●○●	0.00068	0.00055		0.00055		
○●○●○●	0.00072	0.00058	0.00029	0.00029		
●●○●○●	0.00029	0.00023		0.00012	0.00012	
○○●●○●	0.00019	0.00015		0.00008		0.00008
●○●●○●	0.00012	0.00010		0.00010		
○●●●○●	0.00008	0.00007	0.00003	0.00003		
●●●●○●	0.00005	0.00004		0.00002	0.00002	
○○○○●●	0.00643	0.00514			0.00257	0.00257
●○○○●●	0.00166	0.00133		0.00066	0.00066	
○●○○●●	0.00176	0.00141	0.00070		0.00070	
●●○○●●	0.00071	0.00057			0.00057	
○○●○●●	0.00045	0.00036			0.00018	0.00018
●○●○●●	0.00029	0.00023		0.00012	0.00012	
○●●○●●	0.00020	0.00016	0.00008		0.00008	
●●●○●●	0.00013	0.00010			0.00010	
○○○●●●	0.00111	0.00089			0.00045	0.00045
●○○●●●	0.00029	0.00023		0.00012	0.00012	
○●○●●●	0.00031	0.00025	0.00012		0.00012	
●●○●●●	0.00013	0.00010			0.00010	
○○●●●●	0.00008	0.00007			0.00003	0.00003
●○●●●●	0.00005	0.00004		0.00002	0.00002	
○●●●●●	0.00004	0.00003	0.00001		0.00001	
●●●●●●	0.00003	0.00002			0.00002	
		Total	**0.02605**	**0.02605**	**0.01093**	**0.73721**

B 20% ^{13}C-octanoate, 80% glucose model predictions

Fc2		Fc0	Fc1	Fc12
octanoate	glucose	glucose	glucose	glucose
0.200 + 0.026				
0.226±0.003		**0.737**±0.008	**0.026**±0.003	**0.011**±0.002

Figure 4. *A*, Glucose isotopomers and resultant fractional isotopomer contribution to the glucose pool (FC) as generated from TCAsim software using liver data from rats infused with [2,4,6,8-$^{13}C_4$]octanoate for 105 min. Brain energy metabolism was modeled using an 80% glucose contribution (80% of FC) giving rise to acetyl-CoA populations as shown (Fc1, Fc2, Fc12, and Fc0). *B*, By combining 80% glucose contribution with 20% from exogenous [2,4,6,8-$^{13}C_4$]octanoate, 100% of brain energy metabolism is accounted for (not different from steady-state analysis values in Table 1; $p \leq 0.01$).

Discussion

These data demonstrate that a medium-chain fatty acid (octanoate) can directly contribute ~20% of energy for brain in an intact, physiological system. Isotopomer analysis of glutamate versus glutamine indicates that oxidation of octanoate within brain is compartmentalized and associated with the production of glutamine. This compartment is also responsible for the majority of anaplerotic flux that occurs in brain. Additionally, we demonstrated that gluconeogenesis from ^{13}C-labeled octanoate contributes to blood glucose, which in turn is oxidized in brain. On the basis of glucose enrichment data and reinforced by the model, glucose (predominantly unlabeled) and ^{13}C-labeled octanoate can account for the entire oxidative metabolism of brain.

Although glucose is the major oxidative fuel for brain, fatty acids are used as well (Edmond et al., 1987; Auestad et al., 1991; Kuge et al., 1995). Several studies have examined fatty acid metabolism in brain using acetate, the simplest of fats (Badar-Goffer et al., 1990; Cerdan et al., 1990; Hassel and Sonnewald, 1995; Sonnewald et al., 1996; Lebon et al., 2002). However, acetate is not a primary physiological fuel for brain (Vannucci and Hawkins, 1983; Edmond, 1992) and crosses the blood–brain barrier relatively slowly using the monocarboxylate transport carrier, where lactate, pyruvate, and ketones compete for transport (Oldendorf, 1973; Waniewski and Martin, 1998). Medium-chain fatty acids are normally present in plasma at significant levels (Mamunes et al., 1974) and readily cross the blood–brain barrier (Oldendorf, 1971, 1973). In experiments reported here, octanoate infusions in intact rats resulted in plasma octanoate concentrations lower than those commonly achieved clinically with oral dosing of medium-chain triglyceride oil (Dean et al., 1989; Roe et al., 2002).

As demonstrated previously using labeled glucose (Badar-Goffer et al., 1990; Lapidot and Gopher, 1994; Aureli et al., 1997; Sibson et al., 2001) and labeled acetate (Badar-Goffer et al., 1990; Cerdan et al., 1990; Brand et al., 1997), incorporation of ^{13}C-labeled octanoate in brain results in different labeling patterns between corresponding glutamate and glutamine carbons (Fig. 1). This phenomenon is not seen in other tissues using the same infusion of [2,4,6,8-$^{13}C_4$]octanoate (data not shown). Because glutamate is the requisite precursor of both glutamine and GABA, differences in labeling patterns in these three molecules reflect some degree of compartmentation or limited exchange. The labeling pattern of GABA is different from that of glutamine (Fig. 1). This suggests that GABA is being created from labeled glutamate that is partially separated from labeled glutamate that is the precursor to glutamine, perhaps the result of GABA synthesis occurring in GABAergic neurons from a metabolic pool of glutamate.

Isotopomer analysis can be performed on any metabolite in exchange with the TCA cycle. We expected that glutamate isotopomer analysis would provide information about brain metabolism as a whole because it reflects a combination of all TCA cycles in the brain in exchange with a pool of glutamate. The most likely sources of glutamate labeling in our experiments arise from (1) octanoate oxidation in astrocytes contributing to the small astrocytic pool of glutamate, (2) octanoate oxidation in astrocytes

←

resulting in labeled glutamine, subsequently exported to neurons and converted to glutamate by the action of the neurotransmitter cycle, which contributes to the large neuronal glutamate pool, and (3) oxidation of labeled glucose contributing primarily to the large neuronal glutamate pool. Glutamine isotopomer analysis, on the other hand, gives information primarily regarding the astrocytic TCA cycle, because glutamine synthetase is an astrocyte-specific enzyme (Norenberg and Martinez-Hernandez, 1979). Glutamate analysis reflected a 20% enrichment of acetyl-CoA carbon 2 after subtraction of the contribution of enriched glucose, which represents a significant ^{13}C-octanoate contribution to overall brain oxidative metabolism. When glutamine analysis is examined (Fc2 = 56% of the acetyl-CoA pool), it becomes apparent that most of the octanoate oxidation is occurring within a brain compartment associated with glutamine production.

It was expected that octanoate metabolism would take place exclusively in the astrocytes (Edmond et al., 1987) and that glucose oxidation would occur primarily in neuronal cells (Edmond et al., 1987; Magistretti and Pellerin, 1999). Glutamine isotopomer analysis yielded Fc2 values two- to threefold higher than glutamate isotopomer analyses (Table 1), which is consistent with ^{13}C-labeled octanoate oxidation by the astrocytic TCA cycle. Furthermore, the anaplerotic contribution to brain glutamine (39.6 ± 2.6%) was greater than that of glutamate (7.3 ± 3.4%), with *Y* values considerably higher in glutamine versus glutamate isotopomer analysis (Table 1), indicating that most of the anaplerotic flux in brain is occurring in the TCA cycle associated with glutamine production.

NAA was also examined to further investigate compartmentation of brain metabolism. This modified amino acid is a well established neuronal marker (Simmons et al., 1991), and L-aspartate *N*-acetyltransferase, the enzyme that synthesizes NAA from acetyl-CoA and aspartate, is localized in neuronal mitochondria (Patel and Clark, 1979). Under steady-state conditions, it would be expected that enrichment of the acetyl moiety of NAA would give an accurate reflection of acetyl-CoA pool enrichment specifically in neuronal cells. NAA C6 (corresponding to the methyl carbon of acetyl-CoA) enrichment was 8.5 ± 3.4%. This is not different from fractional enrichment of lactate C3 (4.0 ± 0.8%) or of acetyl-CoA C2 (arising from glucose) in brain (Fc2 + Fc12 = 3.9 ± 2.5%). Taken together, these data are consistent with (1) octanoate oxidation and substantial anaplerotic flux in astrocytes and (2) oxidation of glucose [or glucose-derived lactate (Magistretti and Pellerin, 1999)] occurring primarily in neurons.

The overall brain relative anaplerotic flux value reported here (Table 1) is in excellent agreement with previously reported estimations of anaplerotic flux (10%) (Cheng et al., 1967; Aureli et al., 1997). These measurements were made relative to carbohydrate oxidation as opposed to total substrate oxidation. Our experiments indicate that 80% of brain oxidative metabolism is a result of glucose oxidation and 20% is from noncarbohydrate sources. If previous brain estimations of anaplerotic flux on the basis of oxidative use of glucose (Cheng et al., 1967; Aureli et al., 1997) are adjusted to consider anaplerotic flux on the basis of oxidative use of all substrates, this results in a corrected overall anaplerotic flux value of 8%, which is in close agreement with this study (Table 1). Astrocytic TCA cycle relative anaplerotic flux (66%) (Table 1) likely accounts for the majority of brain anaplerotic flux. This is in excellent agreement with a study using acetate to study the glial TCA cycle, which reported that 65% of cycle intermediates were lost per turn, and flux through pyruvate carboxylase was ~60% that of pyruvate dehydrogenase (Hassel et al., 1995).

Although the rate of neurotransmitter cycling has been calculated previously (Lebon et al., 2002), the rate at which metabolites from this cycle exchange with metabolites from the TCA cycle in both astrocytes and neurons is less clear. Certainly this exchange did occur in our experiments, as evidenced by the appearance of substantial quantities of labeled glutamate with administration of ^{13}C-octanoate, a fuel that is specifically oxidized in astrocytes. Without operation of the neurotransmitter cycle, label incorporation into glutamate would have arisen predominantly from neuronal metabolism of the small amount of labeled glucose (~7%) and thus have been substantially lower than that observed. A large portion of relative anaplerotic flux that we ascribe to astrocytes may be to support neurotransmitter cycling through net production of glutamine via glutamate and α-ketoglutarate. However, the proportion or absolute magnitude of anaplerotic flux that is directly linked to the neurotransmitter cycle in this manner is unknown.

Oxidative entry of doubly labeled acetyl-CoA (Fc12) was clearly demonstrated in brain spectra. Because labeled fatty acid oxidized by astrocytes rapidly gives rise to label in glutamine (Badar-Goffer et al., 1990; Brand et al., 1997) and the D45 is not readily visible in glutamine resonances (Fig. 1), it is not likely that the observed glutamate D45 was caused by ^{13}C label exiting the TCA cycle as pyruvate and reentering through acetyl CoA (pyruvate recycling) within the compartment oxidizing fatty acids. Therefore, ^{13}C-labeled octanoate must have been metabolized elsewhere in the animal and ^{13}C label redistributed into a substrate that would be available for oxidation in brain. The likely pathway for this is liver gluconeogenesis. Liver achieves isotopic steady state by 60 min in the intact rat (Gavva et al., 1994); thus flux through combined anaplerotic reactions relative to TCA cycle flux (*Y*) could be assessed accurately. Liver values for *Y* were calculated to be 37%. In liver much of this flux is through phosphoenolpyruvate carboxykinase, leading to subsequent generation of labeled glucose (Jones et al., 1997). On the basis of liver and blood glucose enrichment measurements and their correlation with labeled lactate in brain, additional contribution to labeled acetyl-CoA pool in brain was attributed to ^{13}C-enriched glucose.

It is conceivable that a contribution to Fc2 may have been caused by ketones from liver ketogenesis, which would preserve the labeling paradigm of [2,4,6,8-$^{13}C_4$]octanoate. Several points dispute significant oxidation of ketones by brain under these conditions. First, concentration of ketones at the end of the experiment was 357.4 ± 97.8 μM. Although this represents a 2.7-fold increase over the endogenous concentration, ^{13}C enrichment of ketones was only 22.6 ± 8.1%; the remaining 77% unlabeled ketones would contribute to Fc0 when metabolized, for which there is not much latitude in the data. Additionally, oxidation of octanoate and glucose can account for the entire oxidative metabolism of brain (Fig. 4). If the 80% glucose/20% octanoate metabolic model is shifted to either side of this 80:20 ratio by even 4%, modeled fractional enrichment of acetyl-CoA in brain becomes significantly different from our experimental data (Table 1). Thus, there is very little margin in the data or in the model for additional sources of unlabeled (or partially labeled) oxidizable substrates. Second, ketones are not a primary fuel for brain in fed animals. Hawkins et al. (1971) calculated that only 3% of total brain oxygen consumption in fed, anesthetized rats was caused by metabolism of ketones at an arterial blood ketone concentration of 0.228 mM. Ketone uptake is linear with arterial plasma ketone

concentration from 0 to 1.5 mM (Hawkins et al., 1971). Extrapolation of these data using the highest arterial concentration of ketones measured at the end of our experiment (0.357 mM) showed that ketones contributed <5% to brain metabolism in our animals. With 23% ketone ^{13}C enrichment observed, ketone contribution to Fc2 is at most 1%. Third, unlike octanoate, which is oxidized solely in astrocytes, ketones have been shown to be oxidized by both neurons and glia, albeit to varying degrees (Edmond et al., 1987; Künnecke et al., 1993; Pan et al., 2002). Significant ketone metabolism by both neurons and glia would not explain the dramatic difference between glutamate and glutamine isotopomer analyses (Table 1). Combined, this evidence demonstrates levels of ketone usage in these experiments that are inconsequential to our conclusions.

A recent study that used labeled acetate in human subjects estimated that 14% of brain oxygen consumption was caused by astroglial TCA cycle flux (Lebon et al., 2002). Assuming glial-specific fatty acid oxidation in brain, the 20% contribution of octanoate to brain metabolism reported here implies that the glial contribution to total brain oxygen consumption is at least 20% under these conditions. The higher proportion may be explained by differences in transport rates and mechanisms of the two substrates (Oldendorf, 1971, 1973), or it could be a consequence of anesthesia, fasting, or species differences. Astrocyte-specific metabolism of acetate has been attributed to transport by a monocarboxylate transport-like system (Waniewski and Martin, 1998). Data from this study and others (Edmond et al., 1987) support an astrocyte-specific metabolism of octanoate, which may have cell type-restricted metabolism in brain by a different mechanism, such as expression of β-oxidation enzymes.

In summary, results reported here provide evidence that fatty acid metabolic pathways are active in brain and that octanoate can contribute 20% of oxidative metabolism in brain in an intact, physiological system. Taken together, these data are consistent with octanoate oxidation and substantial anaplerotic flux in astrocytes and with oxidation of glucose primarily occurring in neurons. The data fit well with a simple model in which the combination of octanoate and glucose can account for all of brain energy metabolism.

References

Auestad N, Korsak RA, Morrow JW, Edmond J (1991) Fatty acid oxidation and ketogenesis by astrocytes in primary culture. J Neurochem 56:1376–1386.

Aureli T, di Cocco ME, Calvani M, Conti F (1997) The entry of [1-^{13}C]glucose into biochemical pathways reveals a complex compartmentation and metabolite trafficking between glia and neurons: a study by ^{13}C-NMR spectroscopy. Brain Res 765:218–227.

Badar-Goffer RS, Bachelard HS, Morris PG (1990) Cerebral metabolism of acetate and glucose studied by ^{13}C-n.m.r. spectroscopy. A technique for investigating metabolic compartmentation in the brain. Biochemical J 266:133–139.

Brand A, Richter-Landsberg C, Leibfritz D (1997) Metabolism of acetate in rat brain neurons, astrocytes and cocultures: metabolic interactions between neurons and glia cells, monitored by NMR spectroscopy. Cell Mol Biol 43:645–657.

Cerdan S, Künnecke B, Seelig J (1990) Cerebral metabolism of [1,2-$^{13}C_2$]acetate as detected by *in vivo* and *in vitro* ^{13}C NMR. J Biol Chem 265:12916–12926.

Cheng SC, Nakamura R, Waelsch H (1967) Relative contribution of carbon dioxide fixation and acetyl-CoA pathways in two nervous tissues. Nature 216:928–929.

Dean HG, Bonser JC, Gent JP (1989) HPLC analysis of brain and plasma for octanoic and decanoic acids. Clin Chem 359:1945–1948.

Eckel RH, Hanson AS, Chen AY, Berman JN, Yost TJ, Brass EP (1992) Dietary substitution of medium-chain triglycerides improves insulin-mediated glucose metabolism in NIDDM subjects. Diabetes 41:641–647.

Edmond J (1992) Energy metabolism in developing brain cells. Can J Physiol Pharmacol 70:S118–129.

Edmond J, Robbins RA, Bergstrom JD, Cole RA, de Vellis J (1987) Capacity for substrate utilization in oxidative metabolism by neurons, astrocytes, and oligodendrocytes from developing brain in primary culture. J Neurosci Res 18:551–561.

Gavva SR, Wiethoff AJ, Zhao P, Malloy CR, Sherry AD (1994) A ^{13}C isotopomer n.m.r. method for monitoring incomplete β-oxidation of fatty acids in intact tissue. Biochem J 303:847–853.

Gillingham M, Van Calcar S, Ney D, Wolff J, Harding C (1999) Dietary management of long-chain 3-hydroxyacyl-CoA dehydrogenase deficiency (LCHADD). A case report and survey. J Inherit Metab Dis 22:123–131.

Hassel B, Sonnewald U (1995) Glial formation of pyruvate and lactate from TCA cycle intermediates: implications for the inactivation of transmitter amino acids? J Neurochem 65:2227–2234.

Hassel B, Sonnewald U, Fonnum F (1995) Glial-neuronal interactions as studied by cerebral metabolism of [2-^{13}C]acetate and [1-^{13}C]glucose: an ex vivo ^{13}C NMR spectroscopic study. J Neurochem 64:2773–2782.

Hawkins RA, Williamson DH, Krebs HA (1971) Ketone-body utilization by adult and suckling rat brain *in vivo*. Biochem J 122:13–18.

Jeffrey FMH, Rajagopal A, Malloy CR, Sherry AD (1991) ^{13}C-NMR: a simple yet comprehensive method for analysis of intermediary metabolism. Trends Biochem Sci 16:5–10.

Jeffrey FMH, Storey CJ, Sherry AD, Malloy CR (1996) ^{13}C isotopomer model for estimation of anaplerotic substrate oxidation via acetyl-CoA. Am J Physiol 271:E788–99.

Jones JG, Naidoo R, Sherry AD, Jeffrey FMH, Cottam GL, Malloy CR (1997) Measurement of gluconeogenesis and pyruvate recycling in the rat liver: a simple analysis of glucose and glutamate isotopomers during metabolism of [1,2,3-^{13}C]propionate. FEBS Lett 412:131–137.

Kuge Y, Hajima K, Kawashima H, Yamazaki H, Hashimoto N, Miyake Y (1995) Brain uptake and metabolism of [1-^{11}C]octanoate in rats: pharmacokinetic basis for its application as a radiopharmaceutical for studying brain fatty acid metabolism. Ann Nuclear Med 9:137–142.

Künnecke B, Cerdan S, Seelig J (1993) Cerebral metabolism of [1,2-$^{13}C_2$]glucose and [U-$^{13}C_4$]3-hydroxybutyrate in rat brain as detected by ^{13}C NMR spectroscopy. NMR Med 6:264–277.

Lapidot A, Gopher A (1994) Cerebral metabolic compartmentation. Estimation of glucose flux via pyruvate carboxylase/pyruvate dehydrogenase by ^{13}C NMR isotopomer analysis of D-[U-^{13}C]glucose metabolites. J Biol Chem 269:27198–27208.

Lebon V, Petersen KF, Cline GW, Shen J, Mason GF, Dufour S, Behar KL, Shulman GI, Rothman DL (2002) Astroglial contribution to brain energy metabolism in humans revealed by ^{13}C nuclear magnetic resonance spectroscopy: elucidation of the dominant pathway for neurotransmitter glutamate repletion and measurement of astrocytic oxidative metabolism. J Neurosci 22:1523–1531.

Magistretti PJ, Pellerin L (1999) Cellular mechanisms of brain energy metabolism and their relevance to functional brain imaging. Philos Trans R Soc Lond B Biol Sci 354:1155–1163.

Malloy CR, Sherry AD, Jeffrey FMH (1987) Carbon flux through citric acid cycle pathways in perfused heart by ^{13}C NMR spectroscopy. FEBS Lett 212:58–62.

Malloy CR, Sherry AD, Jeffrey FMH (1988) Evaluation of carbon flux and substrate selection through alternate pathways involving the citric acid cycle of the heart by ^{13}C NMR spectroscopy. J Biol Chem 263:6964–6971.

Malloy CR, Thompson JR, Jeffrey FMH, Sherry AD (1990) Contribution of exogenous substrates to acetyl coenzyme A: measurement by ^{13}C NMR under non-steady-state conditions. Biochemistry 29:6756–6761.

Mamunes P, DeVries GH, Miller CD, David RB (1975) Fatty acid quantitation in Reye's syndrome. In: Reye's syndrome (Pollack JD, ed), pp 245–254. New York: Grune Stratton.

Maughan RJ (1982) A simple, rapid method for the determination of glucose, lactate, pyruvate, alanine, 3-hydroxybutyrate and acetoacetate on a single 20-μl blood sample. Clin Chim Acta 122:231–240.

Norenberg MD, Martinez-Hernandez A (1979) Fine structural localization of glutamine synthetase in astrocytes of rat brain. Brain Res 161:303–310.

Oldendorf WH (1971) Blood brain barrier permeability to lactate. Eur Neurol 6:49–55.

Oldendorf WH (1973) Carrier-mediated blood-brain barrier transport of short-chain monocarboxylic organic acids. Am J Physiol 224:1450–1453.

Pan JW, de Graaf RA, Petersen KF, Shulman GI, Hetherington HP, Rothman DL (2002) [2,4-$^{13}C_2$]-beta-hydroxybutyrate metabolism in human brain. J Cereb Blood Flow Metab 22:890–898.

Patel TB, Clark JB (1979) Synthesis of *N*-acetyl-L-aspartate by rat brain mitochondria and its involvement in mitochondrial/cytosolic carbon transport. Biochem J 184:539–546.

Powers L, Osborn MK, Yang D, Kien CL, Murray RD, Beylot M, Brunengraber H (1995) Assay of the concentration and stable isotope enrichment of short-chain fatty acids by gas chromatography/mass spectrometry. J Mass Spectrom 30:747–754.

Roe CR, Sweetman L, Roe DS, David F, Brunengraber H (2002) Treatment of cardiomyopathy and rhabdomyolysis in long-chain fat oxidation disorders using an anaplerotic odd-chain triglyceride. J Clin Invest 110:259–269.

Rouis M, Dugi KA, Previato L, Patterson AP, Brunzell JD, Brewer HB, Santamarina-Fojo S (1997) Therapeutic response to medium-chain triglycerides and ω-3 fatty acids in a patient with the familial chylomicronemia syndrome. Arterioscler Thromb Vasc Biol 17:1400–1406.

Sibson NR, Mason GF, Shen J, Cline GW, Herskovits AZ, Wall JE, Behar KL, Rothman DL, Shulman RG (2001) *In vivo* ^{13}C NMR measurement of neurotransmitter glutamate cycling, anaplerosis and TCA cycle flux in rat brain during [2-^{13}C]glucose infusion. J Neurochem 76:975–989.

Simmons ML, Frondoza CG, Coyle JT (1991) Immunocytochemical localization of *N*-acetyl-aspartate with monoclonal antibodies. Neuroscience 45:37–45.

Sokoloff L, Fitzgerald GG, Kaufman EE (1977) Cerebral nutrition and energy metabolism. In: Nutrition and the brain determinants of the availability of nutrients to the brain (Wurtman RJ, Wurtman JJ, eds), pp 87–139. New York: Raven.

Sonnewald U, Therrien G, Butterworth RF (1996) Portacaval anastomosis results in altered neuron-astrocytic metabolic trafficking of amino acids: evidence from ^{13}C-NMR studies. J Neurochem 67:1711–1717.

Sulkers EJ, Lafeber HN, Sauer PJJ (1989) Quantitation of oxidation of medium-chain triglycerides in preterm infants. Pediatr Res 26:294–297.

Vannucci S, Hawkins R (1983) Substrates of energy metabolism of the pituitary and pineal glands. J Neurochem 41:1718–1725.

Waniewski RA, Martin DL (1998) Preferential utilization of acetate by astrocytes is attributable to transport. J Neurosci 18:5225–5233.